COMPDYN 2011
III ECCOMAS Thematic Conference on
Computational Methods in Structural Dynamics and Earthquake Engineering
M. Papadrakakis, M. Fragiadakis, V. Plevris (eds.)
Corfu, Greece, 25–28 May 2011

PRELIMINARY DESIGN OF SEISMICALLY ISOLATED R/C HIGHWAY OVERPASSES – FEATURES OF RELEVANT SOFTWARE AND EXPERIMENTAL TESTING OF ELASTOMERIC BEARINGS

George C. Manos[1], Stergios A. Mitoulis[2], and Anastasios G. Sextos[2]

[1] Laboratory of Experimental Strength of Materials, Department of Civil Engineering
Aristotle University of Thessaloniki
e-mail: gcmanos@civil.auth.gr

[2] Aristotle University of Thessaloniki
mitoulis@ civil.auth.gr

[2] Aristotle University of Thessaloniki
asextos@ civil.auth.gr

Keywords: bridges; seismic isolation; knowledge-based systems; software; preliminary design; testing of elastomeric bearings

Abstract. *The preliminary design of seismically isolated R/C highway overpasses is the target of a software based on the current design provisions of Eurocode 8 (Part 2) as well as on engineering decisions included in the expert system. The features of this expert system, which is aimed to facilitate the design of a highway overpass by isolating its deck with the inclusion of elastomeric bearings, are presented and discussed. For such an upgrade scheme a number of successive checks is necessary in order to select an optimum geometry of the bearings. The developed software includes a series of checks provided by Eurocode 8 (Part 2), in order to ensure the satisfactory seismic performance of the selected upgrade scheme. In doing so, the software accesses a specially created database of the geometrical and mechanical characteristics of either cylindrical or prismatic elastometallic bearings which are commercially available; this database can be easily enriched by relevant data from laboratory tests on isolation devices. The basic assumptions included in the software are (a) modeling the seismic response of the bridge overpass as a SDOF system, and (b) only the longitudinal direction response is considered; it is common practice for seismically isolated bridge systems to restrain the transverse movement of the deck by stoppers. Moreover, the results form a number of tests performed in the Laboratory of Strength of Materials and Structures of Aristotle University, verified the quality of the production process of a local producer of elastomeric bearings subjecting production samples to the sequence of tests specified by International Standard ISO 22762-1 (2005). Strain amplitudes larger than 250% resulted in the debonding of the elastomer from the steel plating. Artificial aging resulted in a small increase of the axial (vertical) stiffness and a small decrease of the shear (horizontal) stiffness of the tested bearings. More specimens must be tested to validate further these findings.*

1 INTRODUCTION

Seismic design of structures, in general, involves the conceptual, preliminary and final design [1], the latter being typically prescribed in detail, for most conventional structures, by the existing seismic code requirements. The conceptual design, however, is not, and cannot easily be, encapsulated in codes' provisions; hence, it relies heavily on engineering judgment, expertise and experience. It is therefore quite often the case that the final design, although completely covered by detailed seismic code provisions, is essentially driven by the choices initially made. The same design process described above is also followed in the case of bridge structures, independently of whether they are typical, short highway overpasses or more complex, long and/or curved bridges. Such bridges, although appearing to be relatively simple structures compared to some irregular buildings, may be designed with numerous different configurations depending on a set of performance (in terms of safety and serviceability), economic (including maintenance), constructability or even aesthetic criteria [2]. This gives the designer the flexibility to choose among various structural configurations, and especially among different strategies for the support of the deck on the abutments and piers; a decision related to the use of monolithic or bearing-type connections. On the other hand, the process to select the desired dimensions and the number of the bearings to be used at each support is often time consuming, as it commonly leads to iterative calculations and numerical analyses [3] and multiple design checks against target code-based criteria concerning both the maximum bearing strain and the overall performance of the bridge structure [4][5].

In general though, it can be claimed that no comprehensive procedure has been presented to this date for the optimal (i.e., cost-effective), preliminary design of seismically isolated highway overpasses and bridges. To this end, the present study aims to facilitate the designer of typical overpass configurations [6] in selecting from a smaller, filtered sample of "eligible" bearing sections, and quickly spot the preferable combination of bearing size, type, number, location and cost at minimal computational effort. The decision-making system developed is based on multiple code-based performance criteria [4][5], statistics arising from the construction of 40 km of bridges along the 680 km, newly built, Egnatia Highway in northern Greece [7], engineering judgment and recent research findings as well as ad-hoc laboratory testing, conducted for the purpose of this study. The particular process is also integrated and implemented in a user-friendly software, which permits the quick selection of the bearing scheme for given structural systems and seismic conditions. An effort was made to cover the majority of realistic overpass and simple bridge configurations, and a wide variety of steel laminated elastomeric bearing sections which are most commonly adopted for practical purposes [8][9][10]. The structure of both the Knowledge-Based Expert System (KBES) and the software developed for preliminary design of base-isolated overpasses, together with their validation against more rigorous numerical analysis procedures, is presented in the following.

2 PRINCIPLES OF SEISMIC ISOLATION OF BRIDGE SYSTEMS AND CURRENT CODE PROVISIONS

2.1 Preliminary design

In Europe, seismic isolation of bridges is performed according to the Eurocode 8 - Part 2 [4] and more specifically according to clause 7, which refers to the basic requirements and compliance criteria, analysis procedures and the verification of the isolating system. Annexes J and K of the Eurocode 8-Part 2 also make reference to the laboratory tests required in order to determine the variation of the design properties of the seismic isolator units and to verify the elastomeric bearings under seismic design situations. Similar provisions exist in the

United States. [5]. The Bridge Engineer is also given the choice between commercially available bearings or any other, experimentally tested, rubber bearing suitable for seismic isolation.

In most practical cases, the preliminary design of seismically isolated bridges can be performed using the response spectrum analysis framework prescribed by Eurocode 8, for a simple rigid deck finite element model which adequately provides a first estimate of the bearings' size, number and configuration. It is noted herein, that the rigid deck model is valid for most of the straight isolated bridges with continuous deck, at least in the longitudinal direction, in which the deck actually "floats" along the isolation pier-deck interface. In the transverse direction, however, the deck is in most cases restrained by stoppers (i.e., seismic links) which prevent excessive transverse deck displacements. In both cases though, as long as the displacements are kept below a prescribed magnitude, the system can be reliably assumed to be a single degree of freedom (SDOF).

The process for the design of the seismic isolation of the above bridges, considering a SDOF response, usually follows a series of simple steps, which are not prescribed by most codes [4][5] with the exception of the Indian code specifications [11], but results from fundamentals of the dynamics of structures:

a) calculation of the weight of the bridge per unit length according to the code provisions for the combination of the dead and permanent loading of the bridge (i.e., according to [12] and partly from the variable vertical loading (i.e., 0.2 for highway or 0.3 for railway bridges according to [4],

b) initial selection of the bearings' cross section, the total height of the elastomer and the number of the bearings per support,

c) calculation of the total effective stiffness K_{tot} of the isolation system in the longitudinal direction of the bridge,

d) calculation of the effective longitudinal period of the bridge as $T_{eff} = 2 \cdot \pi \cdot \sqrt{\frac{m_{tot}}{K_{tot}}}$, where m_{tot} is the total mass of the bridge,

e) calculation of the seismic displacement $d_{Ed,x}$ of the deck in the longitudinal direction, by using the elastic spectrum of the code, according to Eurocode 8 specific guidance for seismically isolated bridges and

f) performing a final check to judge the bearing adequacy according to code-based performance criteria.

The most common engineering practice for the final design of the aforementioned bridge systems is given in the following with emphasis on the commonly used Low Damping Rubber Bearings (LDRB).

2.2 Final design

The techno-economical selection of an LDRB bridge isolation system is made so as to satisfy all the design constraints arising from safety-oriented code provisions, but also to maximize performance at the lowest possible cost. This is a complicated problem, and depending on the structural configuration of the bridge, the designer has many design alternatives which require an iterative procedure, involving the repeated analysis and the design of the bridge isolation system until both criteria, i.e. code requirements that ensure both safety and cost-effectiveness, are simultaneously satisfied. Typically, the designer selects an acceptable isolation system for the bridge without considering all the possible combinations of bearing type, size and configuration, and without knowing whether the system selected was the best possible balance between cost and performance. Furthermore, most bridge isolation systems use bearings that are manufactured by international companies. In addition, due to the complexity of the above process and although permissible according to the codes, in most cases the designers are reluctant to use experimentally tested products of the local industry, hence, they lean primarily towards commercially manufactured products of the international market.

3 THE PROPOSED KNOWLEDGE-BASED DECISION MAKING SYSTEM

The methodology presented herein for the preliminary design of base isolated bridges is described in detail. The methodology applies to all bridges isolated with low damping steel laminated elastomeric bearings (LDRBs), with the exception of cases where monolithic pier-deck or abutment-deck connections are combined with bearing-type pier-deck connections. The verification of the methodology is given in section 6 of the paper and shows satisfactory results in straight bridges. The structure of the KBES can be summarized in the following three steps, which also conceptually comply with those proposed by [13].

3.1 Step 1: User Input

A database of commercially available and experimentally tested elastomeric bearings is first compiled consisting of bearings' properties, (i.e. shear stiffness G), shape (i.e., rectangular or circular), rubber and steel plate thickness, height, and width, overall area (A) and dimensions (B_x, B_y or D). Possible bridge structural systems, characterized by different number and length of middle and central spans (L_1 or L_2), that define the total bridge length (L_{tot}) and the mass per unit length (m), as well as initial configurations of n bearings are herein defined by the designer. Seismic hazard is also considered with the most commonly used parameters in mind, i.e. the design seismic acceleration (S_a), soil type and the importance factor of the bridge under study.

3.2 Step 2: Decision process

The second step of the methodology includes the necessary and basic calculations and checks for the seismically isolated bridge. The designer decides the acceptable range for bearing compression (σ_e) where a minimum of 2.0 MPa and a maximum value of 5.0 MPa are proposed by the system itself according to [14]. The limit for the bearing's compression ensures that friction will be adequate to avoid the sliding of the bearing during seismic shear loading, whereas the upper limit is given to ensure that the shear strain due to the interaction between the neoprene and the steel plates under compression will remain at acceptable limits (i.e., $\varepsilon c,d \leq 2.5$ according to Eurocode 8 Part 2). It is noted that this limitation is optional, in the sense that it is not explicitly imposed by the codes, however, it is good common practice. For instance, the vast majority of the bearings used in isolated bridges built along the Egnatia Highway have been designed not to exceed 5.0 MPa in compression. As such, the compression criterion is adopted as the first filter applied to all the bearings checked.

Based on the mass of the bridge, the compression stress (σ_e) is derived as a ratio of the total vertical load acting on each bearing (P_i) over its own area (A). The criterion proposed by Eurocode 8-Part 2 for the calculation of the maximum effective normal stress of the bearing is herein adopted:

$$\sigma_e \leq \frac{2 \cdot b_{min}}{3 \cdot t_t} \cdot G \cdot S_{min} \tag{1}$$

where σ_e is maximum effective normal stress of the bearing, b_{min} is the minimum dimension of the bearing, t_t is the total thickness of the elastomeric, G the shear modulus of the elastomer and S_{min} the minimum shape factor of the bearing layers.

It is noted that this criterion has to be applied to every single eligible bearing, in this case, stored in an external database as will be described in Section 4.1. All bearings that pass this filter are marked as “potentially eligible” and proceed to the next check.

By respecting the desired configuration of the bearings as set by the designer at the beginning of the process, for each bearing that has passed the previous check, the total isolation system stiffness (K_{tot}), its effective period (T_{eff}) and spectral displacement (d_{Ed}) are defined and each bearing is separately checked against seismic actions. The criterion used herein is strain-based, checking the horizontal shear deflections of the bearing given the computed level of vertical loading.

All the bearings that passed the above initial screening process are checked against a set of code-prescribed criteria, involving the normalized shear strain of the bearing due to (a) seismic loading, (b) vertical loading and (c) rotation. Herein, the criterion prescribed in Eurocode 8 is adopted, according to which the maximum total shear strain ε_{td} of the equivalent single degree of freedom system of the seismically isolated bridge should not exceed:

$$\varepsilon_{t,d} \leq 6.0 \tag{2}$$

where:

$$\varepsilon_{t,d} = \varepsilon_{s,d} + \varepsilon_{c,d} + \varepsilon_{a,d} \tag{3}$$

and $\varepsilon_{s,d}$ is the shear strain due to the total design seismic displacement, $\varepsilon_{c,d}$ is the shear strain due to compression and $\varepsilon_{a,d}$ is the shear strain due to angular rotation. The latter is clearly the less critical [4]. Shear strain due to the vertical load combination $\varepsilon_{c,d}$ is of the order of 0.70 for a maximum effective normal stress of the bearing that remains below 5.0 MPa as described above.

The second criterion [4] is that the seismically induced shear strain $\varepsilon_{s,d}$ should be limited to:

$$\varepsilon_{s,d} \leq 2.0 \tag{4}$$

The shear strain of the bearing due to seismic load is computed again for the equivalent single degree of freedom system of the isolated bridge based on its dynamic characteristics and seismic response. Equation (4) can be written in terms of the displacement d_{Ed} of the system under study as:

$$\varepsilon_{s,d} = \frac{d_{Ed}}{t_t} \tag{5}$$

where t_t is the total thickness of the elastomeric and $d_{Ed} = \sqrt{d^2_{Ed,x} + d^2_{Ed,y}}$ $d_{Ed} = \sqrt{d^2_{Ed,x}+d^2_{Ed,y}}$

the SRSS combination o the two horizontal components of seismic displacement. It is noted that, in many practical cases, $d_{Ed,y}$ is negligible, as the transverse movements of the deck are restrained by seismic links. Moreover, it was found that the shear strain due to the total design seismic displacement expressed in eq. (5) is more critical than the $\varepsilon_{t,d} \leq 6.0$ criterion of eq. (2) at least for cases where the compressive stress σ_e is kept within the proposed limits, (i.e., $2.0 < \sigma_e < 5.0$ MPa).

4 EXPERIMENTAL TESTING

An experimental investigation was carried out aiming at establishing the mechanical characteristics of elastomeric bearings locally produced. For this purpose a series of standard tests were performed at the Laboratory of Strength of Materials and Structures of Aristotle University according to the International Standard ISO 22762-1 (2005). Initially, these tests were used as qualification tests for the materials used in the production; that is the neoprene, the steel plates and the adhesion materials and processes. These tests are presented in a summary form and discussed in what follows. Next, in an effort to study the influence of certain parameters in the mechanical characteristics of these elastomeric bearings, the vulcanization process was investigated. Finally, compression and shear tests were also conducted with elastomeric bearings as will be presented in the following subsections.

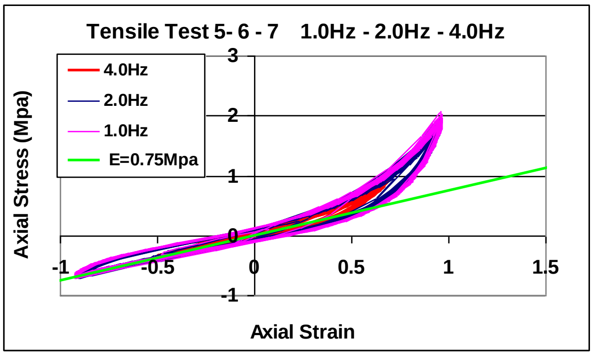

Figure 1a. Tensile cyclic tests with 200% strains

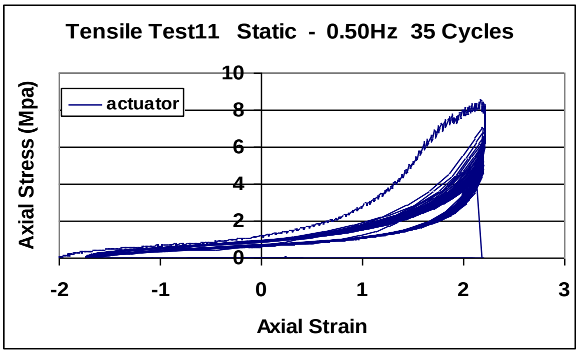

Figure 1b. Tensile cyclic tests with 400% strains that lead to the fracture of the specimen

4.1 Tensile cyclic tests of the neoprene

Eleven tests were performed with frequencies varying from 0.25Hz to 4.0Hz. At the end of the series the specimens failed at maximum axial strain 400% and maximum axial stress 8MPa. At fracture the specimen underwent approximately 500 cycles. The approximate Young's modulus was found to be equal to 0.75MPa. At high levels of axial strain (more than 100%) this value was more than double. At even higher levels of strain this value was further increased. At the initial static load-unload cycles there was a considerable difference in the load-unload path that tended to become less pronounced when the loading cycles increased in numbers. There was no noticeable influence on the behavior of the specimen arising from the frequency of the loading. The cyclic loading was introduced from an initial condition that was the result of preloading it with 50% of the target maximum strain level. Figure 1a depicts the test results for maximum target strain 200% whereas figure 1b depicts similar results for maximum target strain 400% which resulted in the fracture of the test specimen.

4.2 Shear cyclic tests of unit slices of elastomeric bearings

Shear cyclic tests of a specimens made of two unit slices were performed according to the International Standard ISO 22762-1 (2005). For the prismatic specimens each unit slice included a layer of elastomer and two steel plates from a bearing with plan dimensions 200mm x 200mm. The dimensions of each slice of elastomer were 200mm x 200mm and 7.62mm thickness for the orthogonal specimens (figure 2a); for the cylindrical specimens the diameter of the elastomer was 250mm and its thickness 7.62mm (figure 2b) with the appropriate steel plating. Thus, the tested specimens were formed by two slices of elastomer and four steel plates. Each steel plate had a thickness of 2.94mm and sufficient dimensions in plan to have the elastomer attached and to provide enough room for the loading arrangement. Figure 2b and 3a depicts the used loading arrangement. The final slice-specimen was of relatively large dimensions as to be in plan a one to one representations of elastomeric bearings produced by the same process; that is employing identical unit slices and building it up at the desired height with the appropriate number of such unit slices [14]. A dynamic actuator of considerable displacement and force capability was utilized to introduce a series of cyclic shear strain imposed loading sequences to the specimens (see figures 3b). Initially, the series of tests did not exceed a maximum strain level of 100%. Next a series of similar tests introduced maximum shear strain levels larger than 100% up to the failure of the specimen that appeared in the form of debonding of the elastomer from the steel plating. In what follows typical tests results are presented in brief.

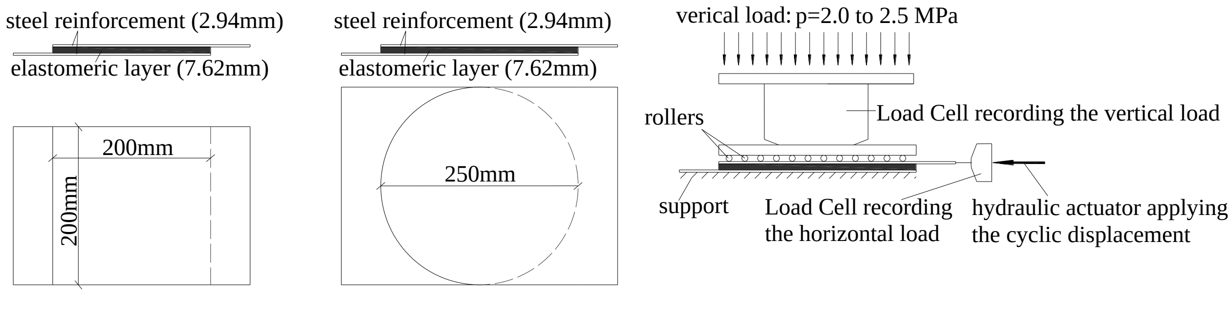

(a) (b) (c)

Figure 2: Cross sections and plan views of: (a) Rectangular specimens (200x200x13.5(7.62)mm) and (b) cylindrical specimens (Ø250x13.5(7.62)mm), (c) testing arrangement.

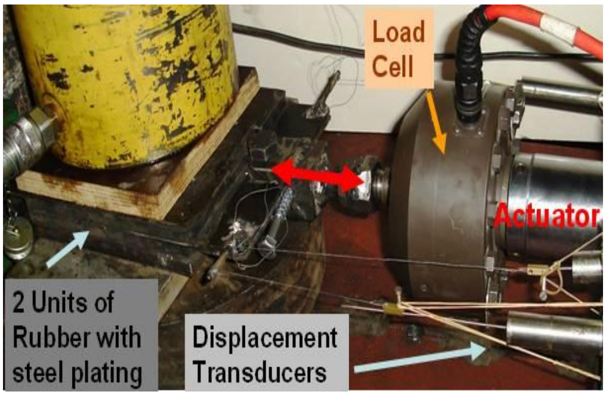

Figure 3a. Loading arrangement of a unit slice.

Figure 3b. Loading arrangement of a unit slice with the simultaneous application of a compressive stress field.

4.2.1. Shear cyclic tests with strain amplitude lower than 100%

Both orthogonal as well as cylindrical geometry elastomeric specimens were tested during this sequence. Throughout all the tests the applied load producing the shear strains was monitored together with the corresponding displacements of the specimen that were utilized to deduce the applied shear stress and shear strain levels to the specimen. At the same time the applied vertical load, normal to the slices of neoprene, was recorded and checked for any significant variations; the objective in this case being to keep the vertical load almost constant at the range of 2.0 to 2.5 MPa throughout all tests. These cyclic tests were performed for the following combinations: 3-11 cycles for each test, with temperature 23 degrees Celsius and cyclic loading varying with frequency 0.2Hz. The shear strain amplitude was varied from 5% to

75% in the following steps: 5% (0.38mm), 10% (0.76mm), 25% (1.91mm), 50% (3.81mm), and 75% (5.72mm). An increase in the shear stiffness was observed when the cyclic shear strain became larger than 75%. Subsequent tests that followed the initial tests with shear strain amplitudes varying again in the range from 5% to 75% exhibited an increase in the shear stiffness when they are compared with the results of the initial shear tests. Again, the specimen exhibited a stable performance throughout the increasing shear strain amplitude from 5% to 75% during these subsequent tests. Additional tests were also performed with the same specimens whereby the studied variable this time was the frequency of imposing the shear strain, keeping the maximum target strain amplitude constant and equal to 75%. The corresponding results are depicted in figure 4a. In this case the specimen's performance was examined for loading frequencies equal to 0.1Hz, 0.5Hz and 1.0Hz. As can be seen from this figure no significant variation in the performance of the specimen could be observed from the obtained response whereby the loading frequency was varied from 0.1Hz to 1.00Hz. An additional specimen of the same geometry and produced by the same process was tested by the loading arrangement shown in figure 3b. This time, apart from imposing the shear strain levels of continuously increasing amplitude, the specimen was placed under a constant compressive stress field normal to the horizontal plane of the elastomer. This stress field corresponded to an equivalent compressive stress equal to 2.4MPa. The frequency of the cyclic load was equal to 0.5Hz and the shear strain amplitude was continuously increasing from 10% to 75%. The summary results of this test are depicted in figure 4b. An increase in the stiffness and a decrease in the equivalent damping ratio is evident when the specimen is subjected to the previously described compressive stress field of 2.4MPMa equivalent uniform stress normal to the elastomer. However, this observation should not be generalized; as was shown from the measurements of another investigation (Ryan et. al. 2004, Manos et. al. 2007) further increase in this compressive stress field has the opposite effect.

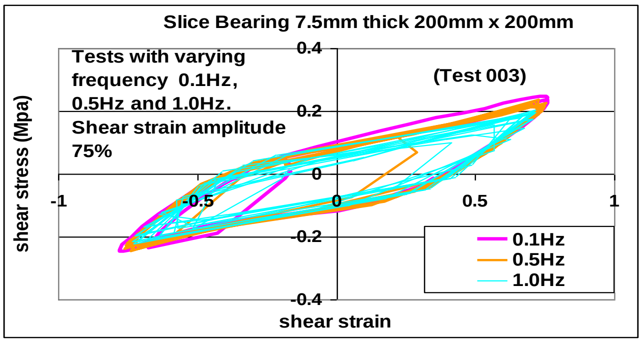

Figure 4a. Shear cyclic test results for shear strain amplitude 75% and frequencies 0.1Hz, 0.5Hz and 1.0Hz

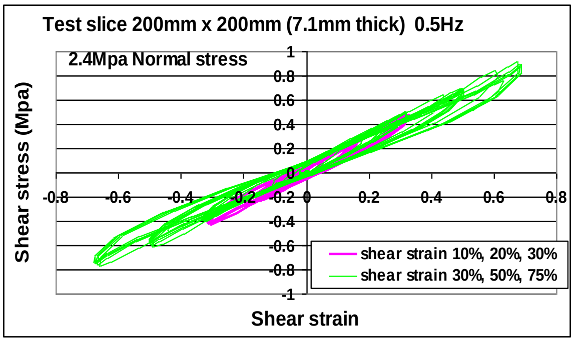

Figure 4b. Shear test results for frequency 0.5Hz and shear strain amplitude from 5% to 75% slice with the simultaneous application of a compressive stress field.

Similar observations can be drawn from the shear test results obtained from the cylindrical geometry specimens. Typical shear test results are depicted in figure 5 whereby a cylindrical bearing slice specimen d=250mm with a variation on the shear strain amplitude up to 90% and the normal stress amplitude (σ) from 0 to 2.0 MPa.

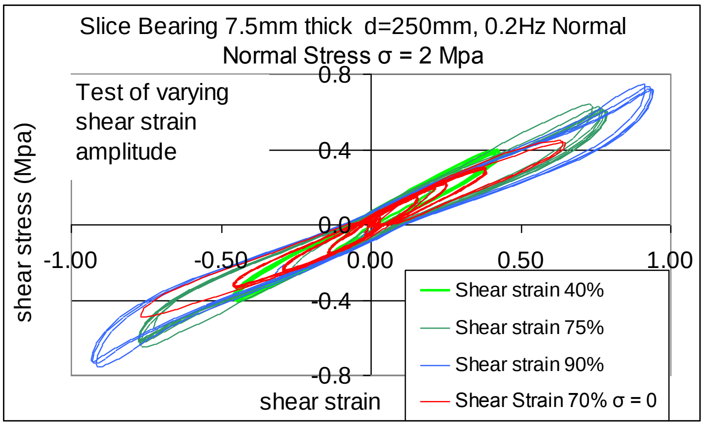

Figure 5: cylindrical bearing slice specimen d=250mm with a variation on the shear strain amplitude up to 90% and the normal stress amplitude (σ) from 0 to 2.0 MPa.

4.2.2. Shear cyclic tests with strain amplitude higher than 100%

The previously described loading sequences were repeated again with unit slice elastomeric specimens of the orthogonal and cylindrical geometry being loaded this time with shear strain amplitudes higher than 100% up to the failure of the specimen. Two distinct loading arrangements were again adopted. First, the shear strains were introduced without the application of compressive load normal to the horizontal plane of the elastomer (figures 2c and 6a) whereas in the second case a vertical load was applied and kept constant producing an equivalent uniform compressive stress normal to the plane of the elastomer in the range of 2.0 to 2.5 MPa (figure 2c and 3b). Figure 6b depicts a typical failing mode during this loading process without the presence of the compressive stress field. Figure 7a depicts the load-unload behavior of this test with large shear strains without the application of compressive normal stress; figure 7b shows the resulting debonding of the elastomer from the steel plating at the end of this loading sequence. The levels of shear strain ranged from 100% and gradually increased to 275%. It can be observed that for shear strain levels lower than 200% the specimen’s behavior remains stable even for this demanding test that corresponds to an elastomeric bearing that does not have the beneficial stabilizing effect of the compressive stress field normal to the slices of the elastomer within the bearing.

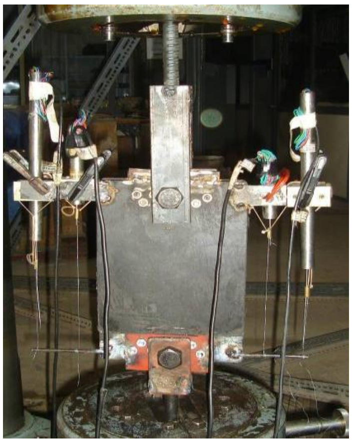

Figure 6a. Loading the unit slice specimen without the presence of the compressive stress field.

Figure 6b. Failing mode of the unit slice specimen without the presence of the compressive stress field.

The maximum shear stress capacity reached for this specimen a value equal to 1.7MPa; this occurred for a maximum strain level equal to 275%. The load-unload behavior of the specimen with the simultaneous application of continuously increasing shear strains and an imposed compressive stress field normal to the elastomer equal to 2.0MPa is shown in figure 7c; figure 7d shows the resulting debonding of the elastomer from the steel plating at the end of this loading sequence. When no compressive field was applied, the level of shear strain reached first a maximum strain equal to 250% whereby the maximum shear stress was observed equal to 1.6Mpa; then for larger shear strain amplitudes the bearing capacity degrades and the specimen reaches its debonding failure mode. The maximum shear stress, when the 2.0Mpa compressive field was applied, reached a maximum value equal to 2.4Mpa for a shear strain level equal to 275%. Then for higher shear strain levels the bearing capacity degrades and the specimen reaches its debonding failure mode. From the comparison of the performance of the specimens with and without the compressive stress field (figures 7c and 7a) it can be seen that the most severe test is that without the normal compressive stress field. It corresponds to an elastomeric bearing that does not have the beneficial stabilizing effect of the compressive stress field normal to the slices of the elastomer.

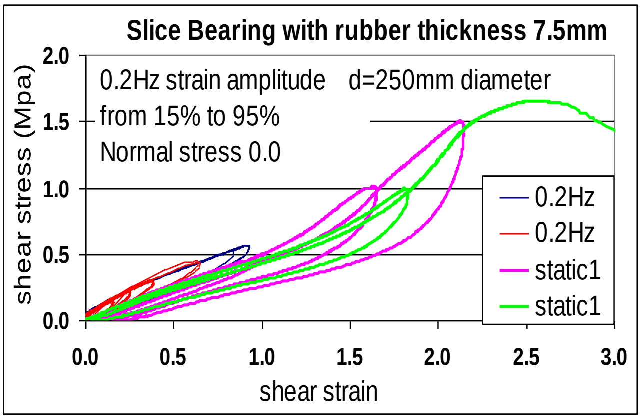

Figure 7a. Shear stress-strain response of the sliced elastomeric specimens up to failure for strains in the region of 300%. (σ=0.0 Mpa)

Figure 7b. The debonding of the elastomer from the steel plating at the end of this loading sequence.

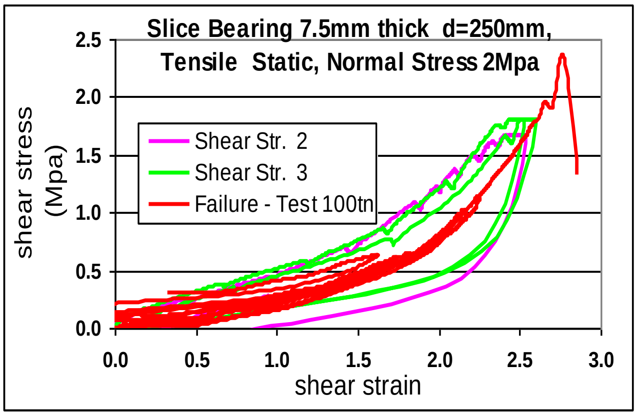

Figure 7c. Shear stress-strain response of the sliced elastomeric specimens up to failure for strains in the region of 300%. (σ=2.0 Mpa)

Figure 7d. Failing mode of the unit slice specimen with the presence of the compressive stress field.

4.3 Tests with elastomeric bearings

After completing an extensive sequence of tests with the slices of the elastomeric bearings, that tried to improve and validate the production process, another sequence of tests was conducted with elastomeric bearings of certain geometry as will be described in the following subsection. This series of tests had as an objective to study the compression and shear behavior of these elastomeric bearings in time and examine the influence on the behavior of an artificial aging process that these bearings were subjected to by keeping them in specific heating conditions for a certain time. Two different elastomeric bearings were examined; the fist was a square bearing with dimensions 150mm x 150mm in plan and a height of 95mm. The clear thickness of the elastomer was 70mm with two layers of elastomer and a thickness of the steel plating equal to 10mm for the outer plates and 5mm for the middle plate. The second elastomeric bearing was again of orthogonal geometry with dimensions 200mm x 250mm in plan having six layers of elastomer. All the steel plating was 3.5mm thick. Two specimens of this bearing were examined; the first had a thickness of the elastomer equal to 72mm (thick) whereas the second specimen had a thickness of the elastomer equal to 57mm. These specimens were subjected to vertical loading tests as well as to test that combined a vertical preloading condition, that resulted to an axial compressive field of approximately 2.0MPa, with a horizontal dynamic load, which produced the desired level of shear strain. The loading arrangement that was utilized is in accordance with the International Standard ISO 22762-1.

4.3.1. Tests with elastomeric bearings 150mm x 150mm

Initially, this elastomeric bearing specimen was tested in compression and then in combined pre-compression of 2.0 MPa and in shear without any artificial aging (23rd September 2008). Then the same specimen was heat treated for 20 days in a temperature equal to 80 C and after cooling it was subjected again to the same loading sequence; e.g. in combined pre-compression of 2.0 MPa and in shear (11th November 2008). During the shear tests, cyclic load was applied with varied frequencies in the range of 0.1 Hz to 1.0Hz. Figures 8a and 8c depict the vertical stress-strain diagram for this specimen before and after the heat treatment whereas figures 8b and 8d depict the shear stress-strain diagram for the same specimen that was first subjected to pre-compression of 2MPa and then to shear strain; again this test was conducted before (figure 8b) and after (figure 8d) the described heat treatment.

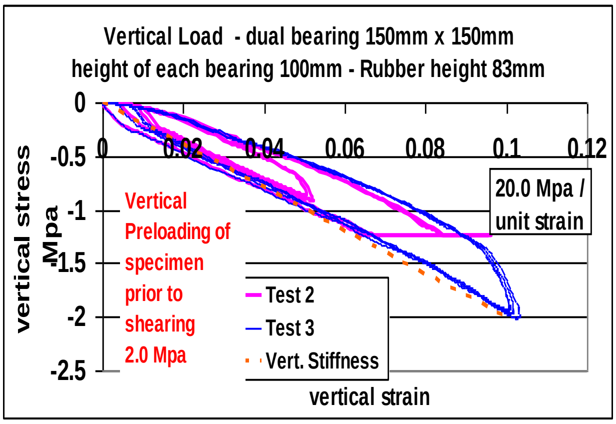

Figure 8a.

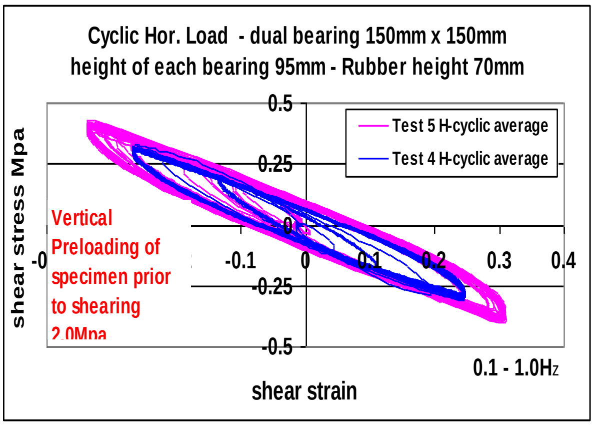

Figure 8b.

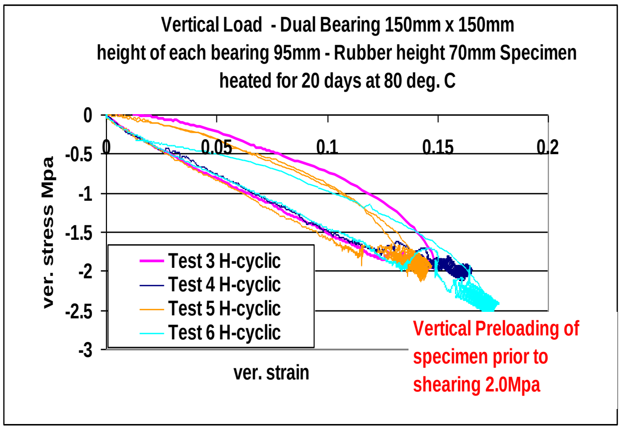

Figure 8c.

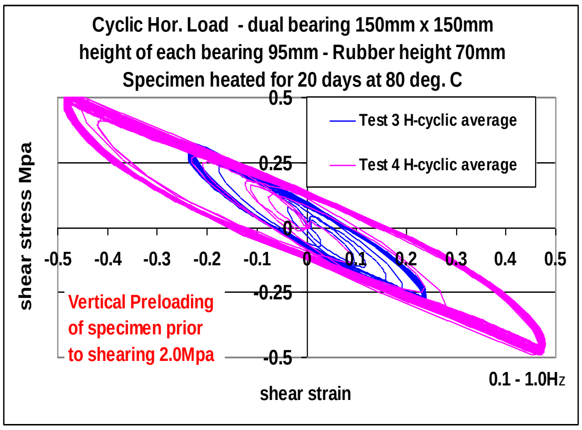

Figure 8d.

Figure 8. Results from compression as well as from combined pre-compression and shear for the elastomeric specimen 150mm x 150mm before and after the artificial aging.

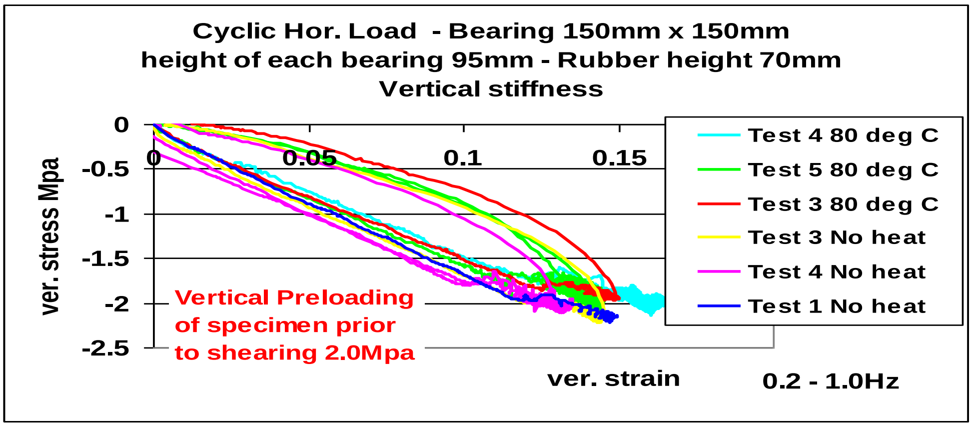

Figure 9. Comparison of the vertical stress-strain response before and after artificial aging.

In figure 9 the comparison of the vertical stress-strain response for this elastomeric bearing specimen before and after artificial aging is shown. As can be seen, this artificial aging process resulted in a small decrease in the vertical stiffness for this elastomeric bearing. In figure 10 the effect of the artificial aging is depicted by comparing the cyclic shear stress-strain response before and after the heat treatment. As can be seen in this figure, this artificial aging process resulted in a very small increase in the shear stiffness for this bearing.

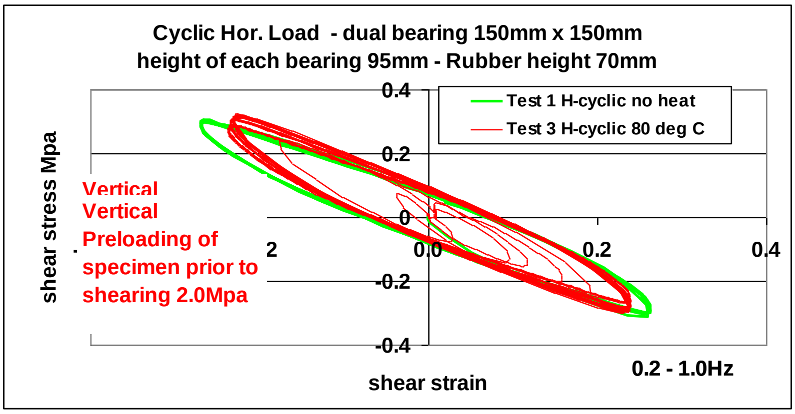

Figure 10. Comparison of the shear stress-strain response before and after artificial aging.

4.3.2. Tests with elastomeric bearings 250mm x 200mm

All the tests for this elastomeric bearing were conducted at the "new" strong reaction frame of the Laboratory of Strength of Materials and Structures of Aristotle University which houses a dynamic actuator with capabilities of ±1000KN in load and ±250mm in displacement and includes servo-electronic control in order to perform dynamic tests in real-time. Figure 11a illustrates a view of this strong reaction frame whereas figure 11b depicts the placement of the elastomeric bearing in this loading arrangement being supported by a special sliding device with very low coefficient of friction.

Figure 11a. The strong reaction frame of Aristotle University.

Figure 11b. The 250mm x 200m elastomeric bearing at the strong reaction frame

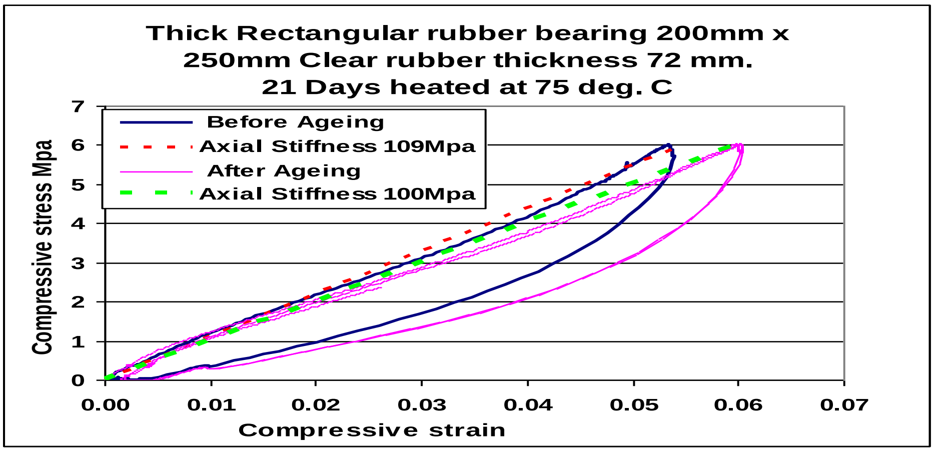

Figure 12. Comparison of the vertical stress-strain response before and after artificial aging.

Initially, this elastomeric bearing specimen was tested in compression and then in combined pre-compression of 6.0 MPa and in shear without any artificial aging. Then the same specimen was heat treated for 21 days in a temperature equal to 75 C and after cooling it was subjected again to the same loading sequence; e.g. in combined pre-compression of 6.0 MPa and in shear. During the shear tests, cyclic load was applied with varied frequencies in the range of 0.1Hz to 0.2Hz. Figures 12 and 13 include summary results of these tests for the specimen with the relatively thick layers of the elastomer (72mm total elastomer thickness). In figure 12 the comparison of the vertical stress-strain response for this elastomeric bearing specimen before and after artificial aging is shown. As can be seen, this artificial aging process resulted in a small decrease in the vertical stiffness for this bearing. In figure 13 the effect of the artificial aging is depicted by comparing the cyclic shear stress-strain response before and after the heat treatment. As can be seen in this figure, this artificial aging process resulted again in a small decrease in the shear stiffness for this bearing.

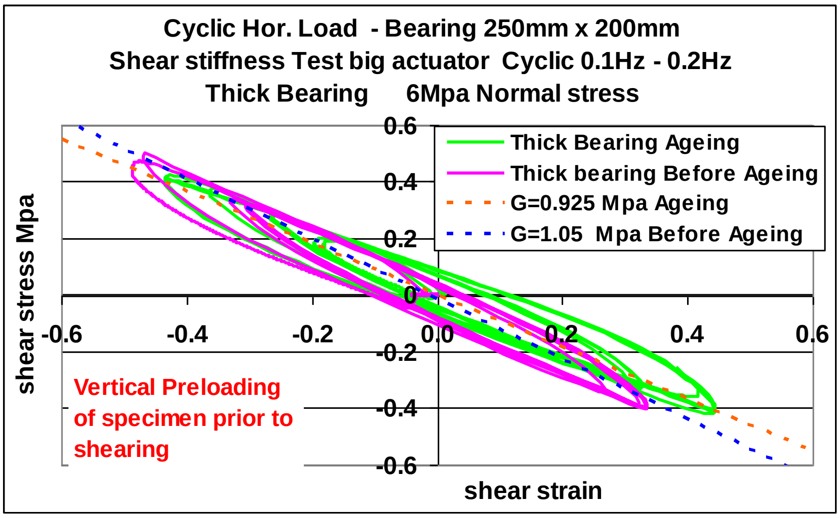

Figure 13. Comparison of the shear stress-strain response before and after artificial aging.

5 SOFTWARE STRUCTURE AND FLOW

5.1 Database structure

The above decision-making system was integrated and implemented in a computer software in order to facilitate the process and visualize the results in a way useful to the designer. As already mentioned, a database of 260 commercially available bearings is developed in Microsoft Access using three distinct relational tables containing the aforementioned necessary fields to describe the bearing geometry and capacity.

5.2 Embedment of non-commercial bearings after laboratory testing

It is noted that the database, which is part of the software, has the ability to be enriched by experimentally verified bearings. This was done for three additional bearings, produced by a local industry, which have been subjected to an extensive testing performed at the Laboratory of Strength of Materials of Aristotle University Thessaloniki. As already mentioned, the experimental study of the present investigation followed the specifications of the International Standards [15], which refer to the properties of the materials of which the elastomeric bearing are composed. These tests involved quality control, vulcanization procedures and construction guidelines and were performed with samples of elastomeric slices taken from the production process. Then, a sequence of prototype tests according to [4] were applied to a series of steel laminated elastomeric bearings produced by the local industry.

The influence of the normal stress level, shear strain amplitude, frequency of shear stress loading and artificial aging was investigated. From such tests the effective shear stiffness and the equivalent effective damping can be deduced together with their variation; the measured values can become input parameters for the developed software [14] [16] [17]. A complete set of the experimental campaign results can be found in [18] [19].

5.3 User input

The main input of the software refers to Step 1 of the proposed methodology and is made through a user-friendly interface which manages previous and new bridge seismic isolation alternative solutions as these are progressively created by the user. A new project, i.e. a new preliminary design of isolation system requires the following input parameters:

(a) **Selection of structural system and bearing type:** The software developed provides for four different bridge structural systems of up to four spans as is illustrated in Figure 6. The first system (Type 1) corresponds to a single span bridge with a length equal to L that is typical for a highway overpass. Type 2 corresponds to an overpass of a higher class of highway with two spans of equal lengths and a middle pier between the lanes of a two-way highway. Types 3 and 4 are alternatives of longer highway bridges. The weight of the superstructure, which essentially controls the vertical load on the bearings, is given by the designer as it is quite possible that the deck section has been selected prior to the selection of the isolation system. A commonly used value of 200 KN/m, is also proposed for cases for which more detailed geometrical data are not available.

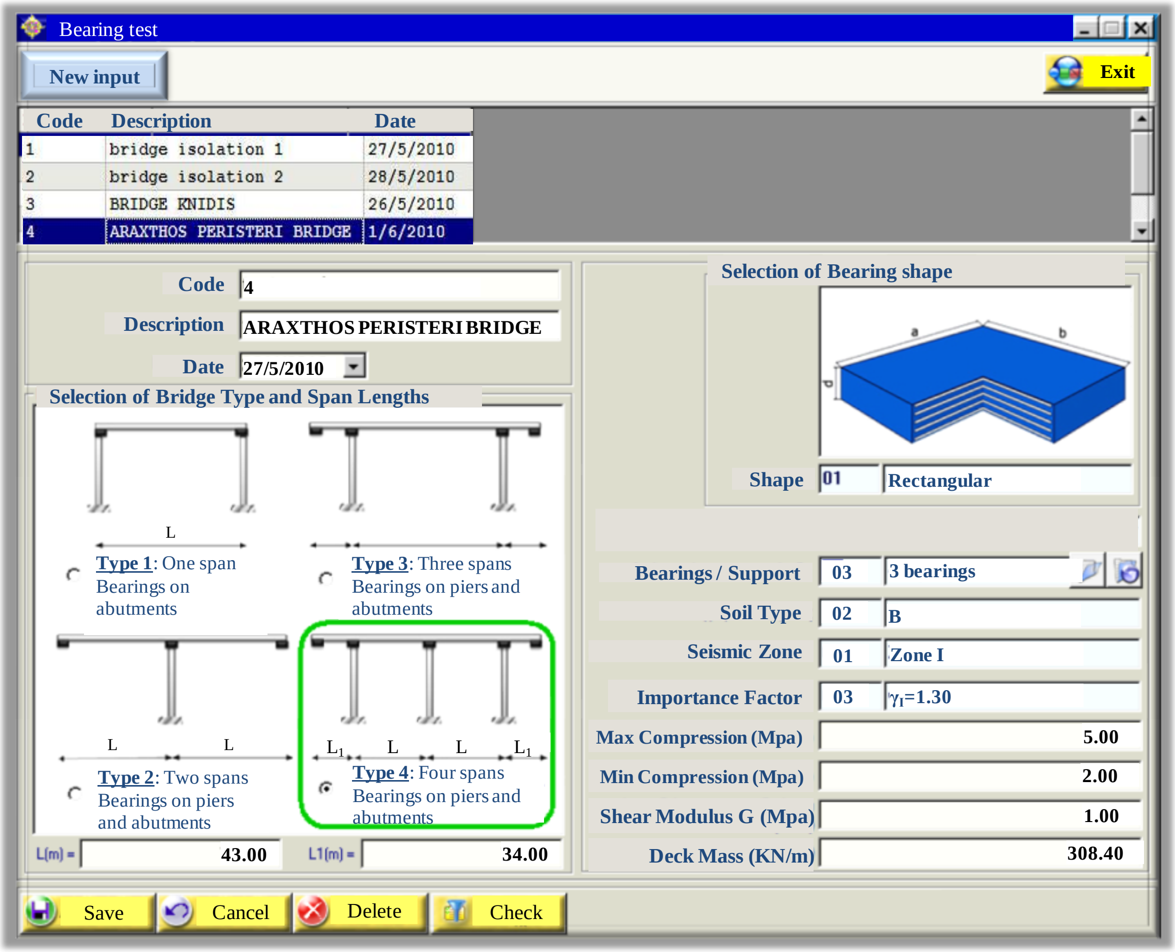

Figure 14: Typical overpass configurations supported by the software developed and overview of the user's interface of the software developed for the preliminary design of bridge isolation system.

(b) Desirable bearing type and configuration: The cross-section of the bearing (i.e., rectangular and/or circular) can also be selected at this stage. In case of pre-stressed and precast I-beam bridge decks, the number of bearings on each support (pier or abutment) is based on the number of the longitudinal beams. In the case of a cast-in-situ box girder or slab-type bridge deck, the number of bearings per support can be decided by the designer as a function of the dimensions of the pier's cap and the anticipated response of the isolated deck as well as making use of the software. As already mentioned, the user can define a minimum and a maximum value for the compression of the bearings or confirm the default range between 2.0 to 5.0MPa. The shear modulus of the bearings is automatically set by the program based on the manufacturer's specifications or any other experimentally justified value for the case of non-commercial bearings after appropriate testing, as described in section 4.2. It is noted that the value generally suggested by Eurocode 8 [4] is 1.0 MPa. However, Eurocode 8 also provides a lower limit of 0.9 MPa and upper limit of 1.5 MPa to be used in two successive analyses that can lead to the maximum displacements or the maximum forces of the isolating system and the bridge piers respectively.

(c) Level of seismic demand: The user defines the level of seismic demand, based on the elastic response spectrum of Eurocode 8-Part 1, the relevant soil classification and importance factor and a peak ground acceleration of 0.16, 0.24 and 0.36 that corresponds to the seismic zonation of Greece; the latter being an open parameter to potentially comply with different levels of seismic hazard in other countries.

5.4 Decision process

The system automatically checks all bearings stored in the database against compression (through the resulting shear strain in the bearing) and the shear strains produced by the earthquake loading based on the compression and shear strain criteria described in Sections 3.2.1 and 3.2.2 and then ranks all eligible bearings that have passed the above checks according to the Optimal Performance criterion. The results are illustrated in a graph, of the $OP_{(i)}$ ratios with the section geometry. The same graph also illustrates the individual safety criterion value ($SC_{(i)}$) and total costs ($CC_{(i)}$) in order to facilitate the designer when making selections based on purely safety or cost criteria. The software also provides in a tabular form the following summary results: (a) the maximum displacement of the deck subjected to the design seismic action, and (b) the aforementioned safety criterion values, cost ratios and optimal performance indicators. Apart from the graph and the table, the software provides an output interface for each eligible bearing, showing the main dynamic characteristics of the analyzed bridge system, i.e. the effective stiffness of the resulting isolating system, the total weight of the superstructure, the effective period of the bridge, the design acceleration at the specific period, the design seismic displacement and finally, a video representation illustrating the fundamental mode of the bridge along the longitudinal direction.

5.5 Assumptions and limitations

The simplified analysis performed in the software considering the rigid deck model for the bridge, is applicable when the total mass of the piers is less than 20% of the total bridge mass, as prescribed by Eurocode 8. The bridges under design should also be straight or have small curvature in plan and small longitudinal inclination. The developed software is not limited by the choice of the deck cross section. The user can employ a default vertical deck load value equal to 200 KN/m, considering that the used combination of loads includes earthquake loading. Otherwise, the user should input an appropriate vertical deck load value if the particular deck does not correspond to the default value. The software can be used in all isolated bridges with elastomeric bearings. However, the software cannot be used in cases when monolithic pier-deck or abutment-deck connections are combined with seismic isolation in the bridge. This structural scheme represents a design alternative implemented in case of long cast, in situ bridge decks or in irregular bridges, which have short piers and are usually protected from the deck's movements through isolation bearings.

As already mentioned, the software is designed for the preliminary design of the isolation of bridges with up to four spans. This restraint is not related with the seismic action, but mostly with the in-service induced movements of the deck, which become significant in bridges with total lengths greater than 150 m according to the limits imposed by various transportation agencies also described by [20]. It was finally decided that the work should be restricted to overpasses and typical small, and intermediate span continuous deck bridges, i.e. with a total length up to, say, 150m.

The bearings are assumed to be actually fixed in their feet, which means that the flexibility of the longitudinal seismic resisting system of the bridge is determined by the flexibility of the isolation. The piers with their foundations were considered to be quite stiff, as compared with the corresponding stiffness of the isolation interface. Therefore, the piers are not considered to participate in the seismic resisting system and they only receive the seismic actions of the bearings supporting the deck. It follows that the software is not recommended to be used in bridges with a flexible pier-foundation system, i.e. in bridges with slender and/or tall piers with flexible foundations. However, it can be underlined that seismic isolation with elastomeric, i.e. LDRB, bearings does not seem to be a design alternative for bridges with flexible pier-foundation systems.

Another assumption of the software concerns the bearings used for the support of the deck to the piers and abutments. The software has the ability to consider a number of bearings per support. This number does not have a restraint due to the calculation procedure used in the software. The software, however, considers that the number of bearings used for the isolation of the bridge deck is the same in all supports, and these bearings are all of the same type, e.g. they have the same cross section area and the same total thickness of the elastomer layers along deck. This assumption is considered to be rational as most bridge structures up to 150m, typically do not use an escalation of either bearings' areas or total thickness of the elastomer.

As far as the seismic action is concerned, the software considers that the isolation system is activated only during the longitudinal design earthquake. The response of the bridge in the transverse direction was assumed to be restrained by seismic links, which join the deck with the piers' heads. This assumption is deemed to be rational, since most bridges with isolated decks use seismic links [4] in the transverse direction, in which the in-service movements, due to creep and/or shrinkage [21] and pre-stressing [22], are negligible. Under the above assumptions, the longitudinal seismic action is transferred to the piers of the bridge through the isolating interface. In the transverse direction, capacity design stoppers transfer the total seismic action directly to the supporting piers without the interjection of the flexible isolation.

6 CONCLUSIVE REMARKS

The knowledge-based methodology developed for the preliminary design of the seismic isolation of bridges is presented in this paper. The proposed methodology is based on the current design provisions of Eurocode 8, but is also complemented by additional criteria set according to expert judgment, laboratory testing and recent research findings, while using a combined cost/performance criterion to select from a database of commercially available bearing products. It also offers the advantage that all possible selections of bearing sections can be considered as potential design solutions as opposed to the common preliminary design procedure, which due to time and complexity constraints investigates a limited number of design alternatives. The methodology is also implemented in a software whose efficiency is validated through more rigorous MDOF parametric numerical analyses as well as by using the case of a real bridge.

It is evident that the prediction success of the preliminary design process, that is proposed here, heavily relies on the extent of the contribution of the fundamental mode in the longitudinal direction, which, when dominant, yields the SDOF simplification as reasonable assumption. To sum up, it is believed that: a) the criteria imposed regarding compression stress limits, which are complementary to the ones prescribed in the codes, b) the automation of the process achieved though the developed software, which permits the investigation of hundreds of different bearing solutions, and c) the eligible bearing hierarchy provided through the proposed safety over cost (Optimal Performance) criterion, provide a significantly large number of potential design alternatives to be considered for the final selection. In this way, the proposed process can be seen as an effective preliminary design tool which is believed to lead to the quicker and more reliable estimate of the optimal bearing selection and seismic response of a highway overpass bridge either in the stage before its final design or when such an existing bridge is checked for upgrading its seismic performance utilizing such an isolation scheme.

The extensive experimental sequence verified the quality of the production process of a local producer of elastomeric bearings by subjecting slices of these bearings, being sampled during production, to the loading sequence specified by the International Standard ISO 22762-1 (2005). As can be concluded from these tests, for shear strain amplitudes lower than 250%, the variation of the frequency and shear strain amplitude did not influence the stiffness and strength properties of the tested specimens. For strain amplitudes larger than 250% the prevailing mode of failure was that of the debonding of the elastomer from the steel plating. Next, the experimental investigation examined the cyclic shear strain performance of locally produced prototype elastomeric bearings by subjecting samples of such bearings to the test sequence specified by the same International Standard ISO 22762-1. This time, the influence of aging was also investigated. As can be deduced from the measured behavior, aging resulted in a small increase of the axial (vertical) stiffness and a small decrease of the shear (horizontal) stiffness of the tested elastomeric bearings. More specimens must be tested to validate further these findings.

7 ACKNOWLEDGEMENTS

This research was conducted in the framework of the Regional Innovation Pole of the Region of Central Macedonia in northern Greece which was established in 2006, in the city of Thessaloniki. The project was funded by the General Secretariat of Research and Technology of the Greek Ministry of Development; its support is gratefully acknowledged. Ms. M. Geraki's contribution in the parametric validation of the software and the help of the personnel of the Laboratory of Strength of Materials and Structures of Aristotle University of Thessaloniki during the experimental tests are also acknowledged. The authors also wish to thank P. Skalkos for his contribution to the development of this specific software.

REFERENCES

[1] Pracasa R. A.V.N.S. BEAS: Expert system for the preliminary design of bearings. Technical Note. Advances in Engineering Software 1992; 14(2): 163-166.

[2] Gavaise E, Papaefthimiou K, Tzaveas T, Stylianidis K, Tegos J. The problem of minimum cost for structural members of earthquake resistant bridges. In Proc. of 5th International Conference of Earthquake Resistant Engineering Structures. Skiathos 2005.

[3] Naeim F, Kelly JM. Design of seismic isolated structures, From theory to practice. John Wiley and Sons, Inc; 1999.

[4] Eurocode 8 - Design of structures for earthquake resistance - Part 2: Bridges, DRAFT No 3. European Committee for Standardization; 2004.
[5] AASHTO. Recommended LRFD Guidelines for the Seismic Design of Highway Bridges. Based on: NCHRP 12-49, Comprehensive Specification for the Seismic Design of Bridges, Revised LRFD Design Specifications, (Seismic Provisions), Third draft of specifications and commentary; March 2001.
[6] Kappos A, Moschonas J. Documented classification of bridges in Greece. Technical Report, Aristotle University Thessaloniki, Greece; 2006.
[7] Konstantinidis D, Maravas A. Egnatia Motorway concrete bridges statistics. In Proc. of 31st ASECAP Study and Information Days, Portoroz, Slovenia 2003; 92-109.
[8] Hamzeh O, Tassoulas JT, Becker EB. Analysis of Elastomeric Bridge Bearings. Report No. 1304-5, Center for Transportation Research, University of Texas, Austin; August 1995: 139.
[9] Kunde MC, Jangid RS. Seismic behavior of isolated bridges: A-state-of-the-art review. Electronic Journal of Structural Engineering 2003; 3: 140-170.
[10] Faravelli L. Modelling the Response of an Elastomeric Base Isolator. Journal of Structural Control. 2001;8(1):17-31.
[11] Indian Railways Institute of Civil Engineering (IRICE), PUNE 411001, Bridge Bearings; 2006.
[12] Eurocode 8 - Design of structures for earthquake resistance - Part 1: General rules, seismic actions and rules for buildings, DRAFT No 3. European Committee for Standardization; 2004.
[13] Pham DT, Pham PTN. Expert Systems in Mechanical and Manufacturing Engineering. The International Journal of Advanced Manufacturing Technology 1998; 3(3):3-21.
[14] Abe M, Yoshida J, Fujino Y. Multi-axial Behaviors of Laminated Rubber Bearings and Their Modeling. I: Experimental Study. ASCE Journal of Structural Engineering 2004; 130(8): 1119-1132.
[15] International Standard ISO 22762-1. Elastomeric seismic protection isolators - Part1: Test methods; 2005.
[16] Kelly JM. Earthquake Resistant Design with rubber. Springer; 1997.
[17] Ryan KL, Kelly JM, Chopra AK. Experimental observation of axial load effects in isolation bearings. In Proc. of 13th World Conference on Earthquake Engineering, Vancouver, B.C., Canada; August 2004; No. 1707.
[18] Manos G, Mitoulis S, Kourtidis V, Sextos A, Tegos I. Study of the behavior of steel laminated rubber bearings under prescribed loads. In Proc. of 10th World Conference on Seismic Isolation, Energy Dissipation and Active Vibrations Control of Structures, Istanbul, Turkey; May 2007.
[19] Manos G, Sextos A, Mitoulis S, Kourtidis V, Geraki M. Tests and improvements of bridge elastomeric bearings and software development for their preliminary design. In Proc of 14th World Conference on Earthquake Engineering, Beijing, China; 2008.
[20] Dicleli M, Albhaisi SM. Estimation of Length Limits for Integral Bridges Built on Clay. ASCE Journal of Bridge Engineering 2004;9(6): 572-581.
[21] Arockiasamy M, Sivakumar M. Design Implications of Creep and Shrinkage in Integral Abutment Bridges. ACI Special Publication 2005; 227(5):85-106.
[22] PCI, Precast, prestressed concrete bridges, the high performance solution, Comprehensive Bridge Design Manual, Accessed online: 1 Dec 2008 (Available via DIALOG. ww.pci.org/publications/bridge).
[23] Mitoulis SA, Tegos IA, Stylianidis K-C. Cost-effectiveness related to the earthquake resisting system of multi-span bridges. Engineering Structures 2010; 32(9):2658-2671.

[24] Seidl G, Weizenegger M. Frame structures in bridge construction. Design, analysis and economic considerations. In Proc. of International Workshop on the Bridges with Integral Abutments. Topics of relevance for the INTAB project, Technical Report 2006:14.
[25] Hawk H. NCHRP 483. Bridge Life-Cycle Cost Analysis. Washington, DC; 2003.
[26] Computers and Structures INC. SAP 2000. Nonlinear Ver. 11.0.4. User's Reference Manual, Berkeley, California; 2002.